Map for the Relaxation Dynamics of Hot Photoelectrons Injected into Liquid Water via Anion Threshold Photodetachment and above Threshold Solvent Ionization

Victor H. Vilchiz, Jeremiah A. Kloepfer, Amy C. Germaine, Victor A. Lenchenkov, and Stephen E. Bradforth*

Department of Chemistry, University of Southern California, University Park, Los Angeles, California 90089-0482

Received: October 26, 2000; In Final Form: January 5, 2001

The early time dynamics of electron photoejection and relaxation after one-photon UV photodetachment of iodide ions in aqueous solution is compared with that resulting from two-photon ionization of neat water. The effect of solvent composition on the ejection and relaxation is probed via experiments on iodide photodetachment in a water/ethylene glycol mixture. Representation of our pump−multiple wavelength probe experimental data sets as two-dimensional contour plots provides a convenient fingerprint of the electron dynamics. Global fitting of the data to a solvation model for spectral evolution indicates varying time scales for solvation for each of the ejection systems. In all cases, the spectral evolution is complete in the first 10 ps, however electrons ejected via the anion charge-transfer-to-solvent pathway relaxes by a factor of 2 slower. For iodide detachment in the water/glycol mixture, evidence is found for a precursor excess electron state in the infrared that decays on the order of 250 fs. No evidence for an electron precursor state is found for the ionization of water within the 400−1000 nm window studied, and the ground state is apparent within 200 fs. From these results, and from picosecond scale recombination dynamics presented elsewhere (Kloepfer et al. *J. Chem. Phys.* **2000**, *113*, 6288−6307), we conclude that the electron production mechanism is distinct for the anion detachment and solvent ionization pathways.

I. Introduction

There has been a recent intensification of research into understanding the dynamics of hydrated electrons, both in the liquid phase[1−6] and in gas-phase clusters.[7−9] This stems from a desire to find and test theoretical models[10−17] that may simulate the dynamics of a quantum solute in a condensed environment. Ultrafast studies of simple dipolar probe molecules have led to some important insights into our understanding of the nature of the solvent response to a change in charge distribution.[18−20] The solvated electron provides a particularly rich testing ground because of the absence of intramolecular degrees of freedom, strong electron−solvent coupling, and large nonequilibrium changes possible when the system undergoes a change in quantum state. It is worth noting that several distinct types of dynamical studies have been performed involving solvated electrons in the condensed phase. The first class aims to uncover and contrast the dynamics of generation of electrons by photoionization from liquid water[4,21−32] and organic solute molecules[33] and by photodetachment from anions such as iodide,[6,34−36] chloride,[37,38] and ferrocyanide.[39,40] Recent studies on electron ejection in low-polarity solvents parallel the experimental work in water. Both ejection via solvent ionization[41] and CTTS ejection from alkali anions[42,43] in these solvents have been explored. The second series of experiments has addressed the solvation and relaxation dynamics after photoexcitation of an *equilibrated* solvated electron into the electronically excited *p* state.[1,2,5,44−46] These experiments, which were pioneered by Barbara's group,[44] address rather different aspects of the solvent response as the solvent cavity is already initially defined and are similar in spirit to experiments that try to understand the relationship between the broad absorption line shape of chromophores in solution with the underlying solvation dynamics. For example, the recent photon echo experiments from Wiersma's group using 5 fs pulses have suggested that the extremely broad absorption spectrum of the equilibrated electron is entirely homogeneously broadened.[2]

The work reported here for the first time critically compares the relaxation of electrons ejected into water by two distinct pathways with high time resolution. Electron photoejection in liquids furnishes a window on a number of fundamental solution phenomena. By use of a short laser pulse, an excess electron is effectively injected into the solvent and the parent species undergoes a sudden change in charge. There is a large rearrangement of the solvent in accommodating such reactions. Depending on the mechanism of the electron ejection, these events may take place within the same solvent sphere as the parent or at separated sites in the solvent. For example, when iodide undergoes photodetachment after resonant excitation into its charge-transfer-to-solvent (CTTS) state,[47] the density for the excess electron is proposed to evolve from an iodine-centered, but diffuse, CTTS cloud to a localized entity at a separate site in the solvent.[48,49] As a result of the electron transfer, the solvent pushes in around the iodine atom[50] and other solvent molecules are expelled from the electron cavity accompanied by the restructuring of the water dipoles around the newly trapped electron. An ultrafast experiment can view the solvent response to these large-scale perturbations.

Further, the solvated electron spectrum has long been known to be exquisitely sensitive to the local solvent structure because of its large spatial extent. Numerous papers on shape stability of the electron spectrum to temperature changes, the changes in the form of the spectrum with increasing ionic strength and

* To whom correspondence should be addressed. E-mail: bradfort@chem1.usc.edu. Fax: (213) 740−3972.

10.1021/jp003974m CCC: $20.00
Published on Web 02/16/2001

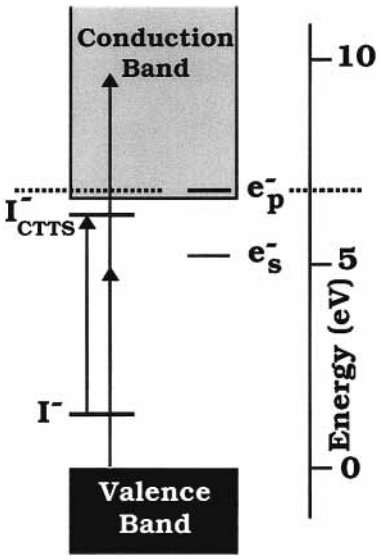

Figure 1. Energy level diagram for the aqueous iodide and neat water systems, based on a figure in ref 58. The positions of the vacuum level (dashed line) and thus the conduction band edge are determined by extrapolation of hydrated electron cluster results and are considerably lower in energy than currently accepted by the radiation chemistry community.[59] The reader is referred to ref 58 for a full discussion of the problems with establishing an energy level diagram for liquid water. In our experiments, the anion is resonantly pumped into the lowest energy edge of the CTTS band, which is below the conduction band. Water is photoionized by absorption of two UV photons putting the excited electron well inside the conduction band. The dynamics of the solvated electrons produced by these two processes are determined by probing the nascent electron throughout its optical spectrum. The arrows indicate the *vertical* excitations to optically accessed states; all other energy levels on the diagram refer to fully relaxed states. The vertical position of the *p* state inside the conduction band on this figure results from the assumptions made by Coe et al. for the location of the conduction band edge.

the addition of cosolvent emphasize how this unusual species provides a window on the local water solvent structure.[51−55] The CTTS state of a halide ion, which is also characterized by a diffuse electronic wave function and is stabilized by the (preexisting) solvent polarization, is known to be extremely sensitive to solvent environment. Recent ab initio calculations confirm that the stabilization energies of the CTTS precursor states in water clusters are indeed sensitive to local solvent structure.[17,56,57] Thus, resolving the dynamics of both the iodide CTTS state and the excess electron itself once injected into the solvent can thus be expected to probe fluctuations and non-equilibrium behavior of the aqueous environment. It is also of interest to consider the change in solvent response to the electron ejection when a cosolvent is added to the water. The microscopic structure and dynamics of hydrogen-bonded solvent shells with admixed solvents has not received much focused attention in the literature to date.

The two pathways investigated and contrasted in this study are the generation and relaxation of photoelectrons following photoexcitation of liquid water itself and of aqueous iodide ions. In the first case, electrons are generated by photoionizing water by two-photon UV absorption (9.7 eV) imparting sufficient energy to reach the bottom of the water conduction band.[58,59] In the case of solute anion detachment, iodide is resonantly excited to the lowest CTTS state with a single 4.8 eV photon, which lies below the threshold for reaching the solvent conduction band (Figure 1).[58] A solvated electron is produced by the solvent-driven breakup of the CTTS state.[13] Past experimental work on multiphoton ionization of water has been interpreted by inclusion of a precursor form of the trapped electron,[26,30,60,61] known alternatively as a pre-solvated, weakly bound or *p*-state[62] electron. This species absorbs in the infrared, peaks at around 1250 nm, and precedes appearance of the ground-state hydrated electron, whose absorption centers in the near-infrared around 720 nm.[30] Recent work has challenged this picture for multiphoton ionization of water,[4,5,63] and it is now clear that the precise number of photons deposited (and thus the excitation energy) is an important parameter in the subsequent electronic dynamics.[21,23] The lifetime of the *p*-state electron is also currently under hot debate.[1,64] In contrast, electrons produced through the solvent induced destruction of the CTTS state are likely to lie below the *p*-state electron (see Figure 1), and thus, this state should not be seen as a precursor if an electron is detached from an iodide ion with a single resonant photon.[11] Therefore, it is of some interest to compare the two pathways for electron ejection to determine the differences in the relaxation of the nascent electron. Furthermore, the electrons generated from the two different pathways may be ejected to different locations in the solvent relative to the parent molecule.[23] In water ionization at energies above 9.3 eV,[23] the electron is believed to spend some time in the conduction band and may reach several solvent shells separation from its parent before becoming trapped.[23,31,65] However, for the electron produced via the lowest iodide CTTS state, quantum simulations suggest that the electron is detached into a ground-state electron and an iodine radical arranged as a contact pair.[13,16] Experimental evidence based on observed geminate recombination dynamics from our lab suggests this marked difference is indeed occurring.[6] This would be expected to lead to differences in the observed relaxation behavior also.

In this paper, we present and contrast early time transient absorption maps of the appearance and spectral evolution dynamics of photoejected electrons produced from solvent ionization and iodide CTTS excitation. For electrons undergoing solvation in water, this requires very high time resolution because of the fast response of water. Our experiments employ state-of-the-art 50 fs deep UV pump pulses; however, because of the broadband nature of wavelengths probed, our experimental time resolution is limited by residual group velocity mismatch (GVM) occurring even in rather thin water jets. The relaxation of electrons after CTTS detachment has not been reported previously. We discuss the effect of modifying the solvent environment on the electron solvation dynamics by looking at the electron ejection from iodide in a solvent mixture of water and ethylene glycol. In fact, only one previous study by Jay-Gerin and co-workers has attempted to globally reconstruct the relaxation of hot electrons generated by water multiphoton ionization,[30] so our results also provide new information on the solvation of an electron after controlled two-photon water ionization. The remainder of the paper is organized as follows. In section II, we describe the experimental procedure; in section III, we present our results and describe how maps of the electron relaxation dynamics are constructed. In the following sections, we describe the solvation model used to globally fit our data sets and the results of this modeling. Finally, we discuss the contrasting dynamics uncovered for the different systems and compare the results for iodide detachment in bulk water with quantum/classical molecular dynamics simulations[13] and time-resolved photoelectron spectroscopy experiments on hydrated iodide clusters.[9]

II. Experimental Section

A detailed description of our experimental setup has been given in a previous publication.[6] Briefly, the pump−probe

experiments presented in this paper are performed using a 200 kHz regeneratively amplified Ti:sapphire laser system (~50 fs pulse width) which drives a 400 nm pumped optical parametric amplifier (OPA).

The 255 nm pump pulses for the photodetachment experiments were obtained by frequency doubling the 510 nm output (35 fs pulse width after optimal prism compression) from the OPA using a ~80 μm thick type-I BBO crystal. A deliberate positive chirp on the 510 nm pulse is optimized using a pair of fused silica prisms in the beam path prior to doubling to yield maximum UV bandwidth and conversion efficiency.[6,66] The resulting UV pulse passes through a pair of calcium fluoride prisms for dispersion compensation. This process results in 255 nm pump pulses of ~50 fs measured by cross-correlation with the 800 nm Ti:sapphire fundamental.[6] The probe pulses for experiments reported here, 450−1000 nm, are obtained from an 800 nm driven white light continuum. In most experiments, the probe color was selected from a portion of the same continuum used to seed the OPA using an interference filter (25 nm bandwidth for the range 450−700 nm, 40 nm bandwidth for 800−1000 nm). The selected color was passed through a pair of fused silica prisms to compensate for group velocity dispersion in the generated white light and the optics later in the probe path. The cross correlation of 255 nm with the probe pulse prepared in this way was measured by difference frequency generation at the sample position using a 90 μm type-I BBO crystal. The cross-correlation ranges from 70 to 85 fs for the various probe wavelengths.

In later experiments, a simpler optical arrangement was employed, albeit at the sacrifice of some time resolution. A separate white light continuum generated in sapphire was formed just prior to the sample, and an interference filter preselected the probe color of interest immediately before the sample; no probe chirp compensation was performed. In this way, data for several additional probe colors could be collected rapidly. In addition, a 0.15 m single monochromator (5−20 nm band-pass depending on probe wavelength) was used just prior to the detection photodiode. It was noticed that, for wavelengths close to the continuum driving frequency (800 nm), if the presample interference filter was removed and the entire continuum was transmitted through the sample (as carried out in a number of other workers' broadband experiments[4,33]) rather different decay profiles were recorded. It appears that it is imperative to exercise caution with probe colors in the near-infrared from a Ti:sapphire fundamental driven continuum, particularly if the entire continuum is dispersed onto a CCD device. Finally, a data set was recorded using the second harmonic of the Ti:sapphire amplifier at 400 nm as a probe. The 255/400 nm cross-correlation was determined to be 85 fs by difference frequency generation.

The relative arrival of the pump and probe pulses is computer controlled by a mechanical stepping translational stage in the probe path. The sample is a free-flowing jet, ~200 μm in thickness, of either an aqueous 60 mM KI (Mallinckrodt) solution, 170 mM KI in a 40 vol % ethylene glycol/water solvent mixture or neat deionized water at room temperature. The pump intensity was varied between 6×10^9 and 2.5×10^{10} W/cm^2 for experiments on I^- and water as described previously.[6,34] The transmission of the probe beam through the sample is detected by a silicon photodiode and processed by a lock-in amplifier referenced to a mechanical chopper in the pump path. In addition, two reference photodiodes monitor pump and probe for laser fluctuation normalization purposes. The 200 kHz repetition-rate pump−probe apparatus yields a high signal-to-noise measurement of the change in probe absorption across a broad range of time delays, but because of the extremely small fractional change in transmission, *absolute* absorbances in the probe beam are not obtained. For this reason, as well as probable variations in the probe interrogated pumped sample interaction volume between runs, we cannot cleanly compare probe absorbances *between* experiments using different probe colors. This is handled by matching the measured signals to the known absorbance of the product electron once its spectrum is fully developed (see below). Data were collected at probe wavelengths in the 400−1000 nm range for the iodide/pure water system at 50 nm intervals and over a 500−1000 nm range for neat water and iodide/solvent mixture in 100 nm intervals.

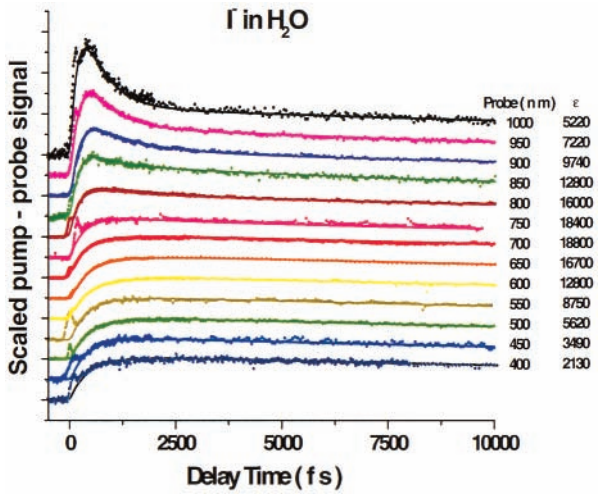

Figure 2. Raw experimental data (circles) obtained from the electron photodetachment of aqueous iodide ions via resonant excitation into the CTTS band. All signals represent a pump-induced absorption for the probe. The solid lines represent the sums of exponential fits used to provide a functional representation of the data. Data for each probe wavelength were recorded in separate experiments. Accurate estimates for the relative optical densities between probe wavelengths are not easily obtainable from the experiment, so all data sets are scaled so that the signals have a common intensity at 10 ps. Finally, the data sets are offset vertically in even intervals for clarity of presentation. The column of values at the far right are the *literature* molar absorption coefficients for the solvated electron; these are subsequently employed to reconstruct the full time-resolved transient absorption spectrum shown in Figure 3.

III. Results

Figure 2 shows the early-time results for probes ranging from 400 to 1000 nm after electron photodetachment from iodide in aqueous solution. Each raw experimental signal has been scaled to have the same magnitude at 10 ps to allow clear comparison. The pump-induced absorbance is largest for probe wavelengths around 700 nm and weakest at 400 and 1000 nm as is evident in the relative signal-to-noise ratios. The pump intensity is set so that less than 5% of the observed electrons originate from ionization of the solvent itself.[6] The raw data presented shows only the first 10 ps of the dynamics; data sets for nearly all probe wavelengths were in fact recorded up to 400 ps (not shown). Signals over the full time range have been reported elsewhere for two probe wavelengths.[6] All long-lived signals observed are expected to originate from a separated electron; we do not expect significant absorption from the iodine radical at any wavelength probed. The initially excited charge transfer-to-solvent state itself may have a fleeting transient absorption spectrum, but this will be extremely short-lived (see below).

The following observations can be made by inspection of the 13 curves shown in Figure 2. The time for the transient

absorption due to the separated electron to rise to its maximum value slows as the probe wavelength is tuned to the blue. The signal rises with a characteristic time scale of ~80 fs at 1000 nm but is biphasic for the blue probe wavelengths. We note that for all probes the extracted rise times are significantly slower than the corresponding pump−probe cross-correlation. Despite the thin water jet used in the experiments, the factor limiting time resolution is the GVM between pump and probe in the ~200 μm thickness jet. Attempts at employing still thinner jets have so far led to poor jet stability. With a 200 μm jet, the calculated GVM ranges between 90 fs for 255/400 and ~105 fs for the 255/1000 experiments using the optical dispersion equation for liquid water.[67] However, we have verified that even with a 1000 nm probe, the observed rise time for the electron is slower than the minimum resolvable feature (~ 100 fs). In parallel with a slower rise in absorption with the bluer probes, probe wavelengths between 750 and 1000 nm manifest a rapid decay; the fastest is at 1000 nm (~ 650 fs). By 6 ps, the spectral evolution is complete and all traces now follow an identical slow decay that reflects electron population loss by geminate recombination. These longer time scale dynamics have been analyzed elsewhere;[6] we therefore focus our attention on the signal rise and spectral evolution dynamics.

These results are most usefully consolidated for presentation in the form of contour plots as a function of time delay and probe wavelength. These contour plots are constructed from mathematical fits to the experimental data and by scaling each probe wavelength data set so that the long-time absorbance matches a known equilibrated absorption spectrum for the solvated electron. In some detail, this reconstruction proceeds as follows: The collected iodide data is fitted with a sum of two exponential rises and multiple exponential decays, convoluted with the appropriate instrument response function, using a nonlinear least squares algorithm to provide the best functional representation of the data. During the fitting scheme, the zero-delay time is treated as a fitting parameter. The simple mathematical form employed implies *no physical model* and is chosen to best represent the data in an unbiased fashion. Once the fits were completed, the signal intensity of each time-resolved trace was scaled so that the transient absorption spectrum at 10 ps matches the literature absorption spectrum for the fully equilibrated electron.[53,68] At this time delay, it is determined from the raw data that the thermalization and relaxation processes are complete and the dynamics from 10 ps on captured in our experiment are only due to population loss and thus the same for all probe wavelengths. The choice of a later delay time has no effect on the reconstructed two-dimensional data sets. A similar spectral reconstruction procedure was used by Hertwig for the relaxation of the solvated electron in photoionization of water[4] and is commonly used for fluorescence spectral evolution.[18,19] This is reasonable on the basis of results for pure H_2O[3] and for D_2O multiphoton ionization,[30] where the transient absorption spectrum is directly measured for electrons undergoing thermalization. Further discussion regarding the validity of this approach will be presented below. We note that during the first 10 ps, no separation of time scales for spectral evolution and population decay is being assumed.

Figure 3a is a representation of the overall spectral evolution dynamics from the raw data using the spectral reconstruction method just described. The key point is that to reconstruct accurate intensities along the spectral axis, each time-domain curve in Figure 2 is scaled by the appropriate factor shown at the right of that figure, which is the extinction coefficient for

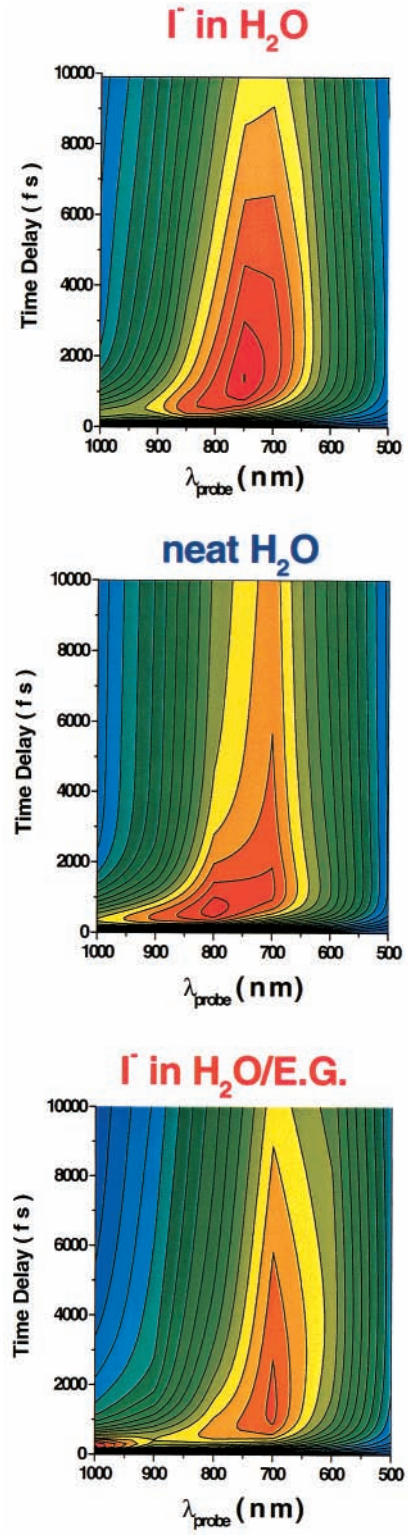

Figure 3. (top) Contour plot constructed using the mathematical fits to the raw data for detachment of aqueous iodide ions shown in Figure 2. The contours displayed are in even intervals over the range of induced probe absorption from blue (zero) to red (highest absorbance). (middle) Similar representation of experimental data for the two-photon ionization of water. (bottom) Representation of the experimental data resulting from resonant excitation of iodide ions into the CTTS-state in a solvent mixture of water and ethylene glycol. Notice the intense feature at early times around 1000 nm. For each contour plot, the transient absorption for each probe wavelength has been matched at 10 ps (15 ps for mixed solvent) to the appropriate literature equilibrium electron spectrum (see text). This assumes the thermalization process is complete by this delay time and no further evolution of the transient spectrum is expected.

the fully equilibrated solvated electron at that probe wavelength. Thus, for all but the earliest delay times, the probe absorbance is largest around 700 nm as observed experimentally. Further, the effect of different time offsets in each separate experiment and the instrument response function are removed in the reconstruction. The contour plot quickly captures the information content of Figure 2 as well as providing a useful comparison for the relative absorption intensities at different probe wavelengths. Two major features are emphasized: (1) A smoothly curved ridge in the plot indicates exponential shifting of the electron absorption spectrum toward the blue with delay time. This shift appears to be completed in ~6 ps and is followed by the onset of an overall absorption decay at all probe wavelengths. (2) The rise in the transient absorption, although delayed, is most rapid at 1000 nm, and the rising edge slows as one inspects the contour plot toward bluer probes.

Experimental data was also recorded for two-photon ionization of neat water pumped at 255 nm. Reasonable signal-to-noise for direct water ionization is obtained by increasing the pump intensity by a factor of 4.[6] Once again, spectral evolution is determined to be complete by 10 ps. Figure 3b shows the reconstructed contour plot obtained from the experimental data sets (not shown) between 500 and 1000 nm. The ejected electrons show a similar spectral evolution throughout the probed region; however, the time scale is clearly more rapid than that seen in Figure 3a. The absorption maximum shift in this case appears to be completed within ~3 ps. The rise time of the absorption at the reddest wavelength measured is 170 fs, similar to that found for iodide. However, the rise times on the blue side of the spectral range are faster, and the decay times on the red side are significantly faster, consistent with a more rapid spectral evolution for the photoelectron ejected from a water molecule.

To probe the effect of the solvent environment on the ejected electron relaxation, the iodide photodetachment dynamics were also monitored in an aqueous solvent mixture: a 17% mole fraction mixture of ethylene glycol in water. This introduces several changes to both the spectroscopy and dynamics of the detachment. The absorption spectrum of the iodide in the mixture is shifted from 225 to 220 nm compared to a pure water environment.[47] Because the experimental pump wavelength employed in these experiments is at the reddest edge of the absorption band, the extinction coefficient in the mixed solvent is markedly lower. Thus, the concentration of iodide was accordingly adjusted to attain a similar optical density as that in the aqueous system. The equilibrium solvated electron spectrum also blue shifts in this solvent mixture; the band center for solvated electrons is estimated to be 676 nm from the data of Idriss-Ali and Freeman (cf. 720 nm in water).[68] The data of Idriss-Ali and Freeman for the entire equilibrated electron spectrum[68] in the solvent mixture is used to normalize signal intensities, at a delay time where the spectral evolution apparent in the raw data is fully complete (in this case at 15 ps), to construct the contour plot (Figure 3c).

The contour plot of detachment in the solvent mixture has some similarity with those described earlier, the solvated electron band undergoes a blue shift in the 900 → 600 nm region. This shifting is slower than in aqueous iodide, and it takes approximately 10 ps to complete. However, an additional island in the infrared at very early time is observed in Figure 3c of comparable intensity to the main band. The 1000 nm data set shows a qualitatively different pump−probe signal: an additional component of significant amplitude characterized by a rapid rise (<180 fs) and almost as rapid decay (~250 fs) is

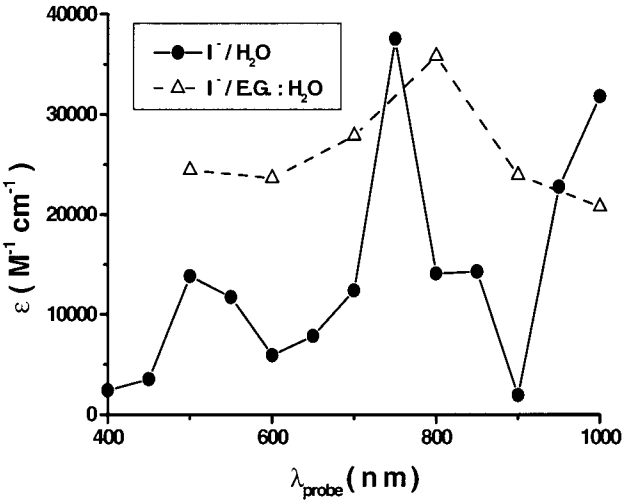

Figure 4. Transient spectrum of the feature appearing in each experimental data set at zero delay after excitation into the iodide CTTS band (see Figure 2). (circles) Detachment of I^- in pure water; (triangles) detachment of I^- in 17% mole fraction ethylene glycol/water mixture. This feature decays with close to our instrument response. Relative intensities are calculated by ratios with the transient absorbance observed at 10 ps for each probe data set and then scaled by the appropriate extinction coefficient of the fully equilibrated solvated electron (see text). This zero-delay feature is not included in the contour representations.

observed in addition to slower decay phases. From the contour plot, this appears like a distinct transient absorption band; however, we do not have data at longer probe wavelengths to confirm definitively this assignment. The possible origin of this feature is discussed in section VI.

A feature present in all of the experimental probe traces for iodide detachment is an absorptive transient around time zero (see Figure 2 or ref 34). The amplitude of this transient, relative to the solvated electron signal, varies with probe wavelength, and scales linearly with iodide concentration (at least at 550 nm). We therefore attribute the transient as originating from a pump−probe interaction with the anion. The amplitude of the transient for I^- in the solvent mixture is greater than in water. However, excitation of the pure solvent also yields a zero-time feature, as noted by a number of authors.[4,30,69] These have been assigned to coherent cross-phase modulations, two-photon absorption, or transient Raman signals, in all cases requiring the simultaneous presence of the pump and probe at the sample. These coherent artifacts for pure solvent can be either positive or negative, have complex shapes, and are sensitive to alignment.[70] However, this is not the case in the observed time-zero features for our iodide data. At each probe wavelength, the feature can be fit with an exponential decaying function ($\tau \sim$ 50 fs) that is instantaneous with the pump. We have chosen to remove the time-zero transient from the reconstructed contour plot. Figure 4 shows the absolute absorbance of the zero-delay peak as a function of probe wavelength. The extinction coefficient was obtained from the ratio of the fitted peak height to electron absorbance at 10 ps, which is calibrated against the known extinction coefficient for the solvated electron at each probe wavelength. The early time transient has the largest extinction coefficient at 750 nm but shows additional spectral structure at least in pure water where we have a larger number of probe wavelengths. It is tempting to assign these spectral features as excited-state absorption (from the CTTS state) to other quasibound CTTS states[10,71] and into the continuum,[72] but a solid assignment and an explanation for the structured transient absorption spectrum is certainly required. Given that our

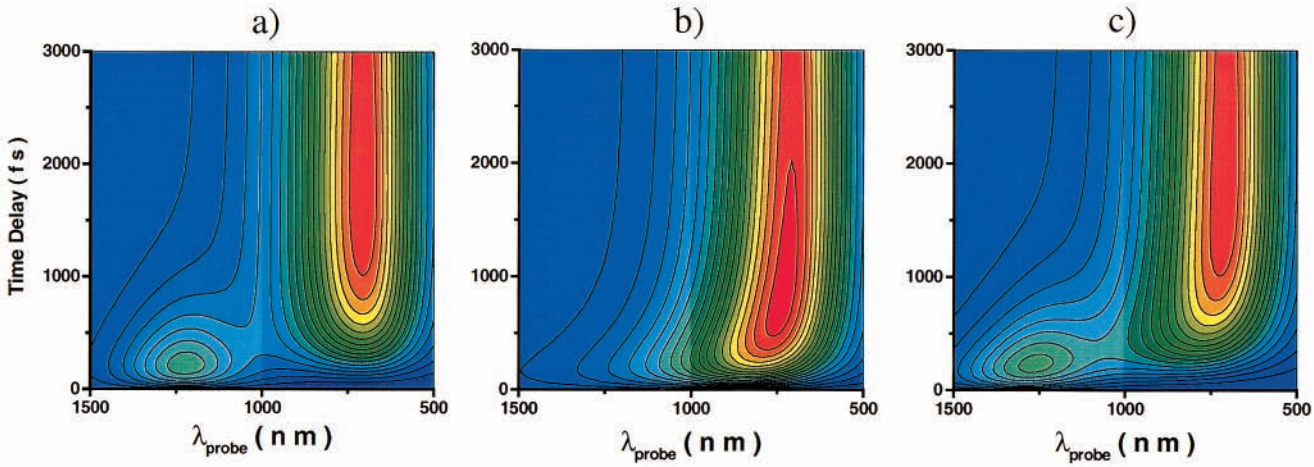

Figure 5. Simulation of electron relaxation resulting from three scenarios. (a) A two-state system where all electrons are trapped in the excited *p* state, band centered at ~1250 nm, then undergo internal conversion to the ground *s* state with band centered at 720 nm. (b) Single electronic state (ground state) undergoing spectral shifting due to solvation dynamics. (c) A two-state system undergoing internal conversion and ground-state solvation. The parameters used in these figures are taken directly from fitting the multiphoton ionization of D_2O, in ref 30: for a and c, the internal conversion time is 410 fs; for b and c, the spectral shift for ground-state electron is ~0.36 eV with an exponential correlation time τ_{corr} of ~510 fs. The trapping time is 160 fs throughout. The opaque spectral region between 1000 and 1500 nm is not probed in the current experimental study.

effective instrumental response due to GVM is ~100 fs, if this feature is assigned to absorption due to the real excited-state population, we are unable to recover an accurate lifetime. We note that the transient has a pronounced polarization anisotropy, unlike the later signal which is due to the trapped electron, whose absorption exhibits no anisotropy throughout the entire time range measured.

IV. Physical Model

Our main goal is to model the relaxation of an electron detached from an anion CTTS state manifested in its spectral evolution and contrast the result with the photoelectron ejection dynamics from water. To facilitate this comparison, the relaxation dynamics of the ejected electron after photoionization from water have been intensively studied by four groups; varying relaxation models have been proposed to account for the observed dynamics.[3,4,30,63] We note that our experiment on the water photoionization process does provide the highest time resolution study to date, and thus, our results provide additional tests of these models. In contrast, no previous study of CTTS ejection looks at the relaxation of the detached electron.

In our comparison, we chose to employ the most general model for electron relaxation proposed by Jay-Gerin and co-workers for the multiphoton ionization of water. This model comprises two states for the electron population with internal conversion between levels and includes spectral evolution of both populations undergoing solvation.[3] The solvation dynamics is not included via an ad hoc kinetic model[5,63] but rather by established treatments for polar solvents rearrangement after a change in charge density.[19] We note that shape stability,[4,55,73] i.e., constant spectral width and overall oscillator strength, is imposed for each electron spectral component while undergoing spectral evolution. The two states are identified with strongly and "weakly bound" electrons;[30] these are often associated with the *s*- and *p*-type states, respectively, arising in the cavity model for the solvated electron based on hybrid quantum classical molecular dynamics simulations.[74] It has been suggested that electrons produced by photoionization of water have sufficient energy to access the weakly bound state that subsequently undergoes internal conversion to the ground state.[26,60−62] Both the lifetime of the *p*-state[64] and whether it is formed in the *photoionization* step has recently become controversial,[4,5,63] and this topic is discussed further in the section VI. Several simulated scenarios are presented in the form of contour plots in Figure 5 illustrating the expected fingerprints of (a) ejection into the *p* state followed by a pure two-state internal conversion, (b) direct ejection to the ground-state and solvation dynamics in the ground state, and (c) ejection into the *p* state accompanied by internal conversion and solvation dynamics in both states. The parameters for these simulations (given in the caption) are those fitted in the work of Jay-Gerin and co-workers for multiphoton ionization of D_2O.

As seen in Figure 5 parts a and c, the *p*-state absorption spectrum is centered near 1250 nm but extends out to 1000 nm,[26,30] mostly beyond the range of probe wavelengths employed in our current study. The form of our experimental data for detachment and ionization in water (Figure 3 parts a and b) is dominated by continuous blue shifting arising from solvation dynamics, most reminiscent of the process depicted in Figure 5b. If one includes the contribution of the *p*-state internal conversion and solvation dynamics in the *s* state (Figure 5c), there are only subtle changes observed if the experimental window extends only to 1000 nm. Because it is difficult to conclude based purely on the experimental data for the necessity for the *p*-state inclusion, as argued by two recent studies of water ionization using similar excitation energy to ours,[3,4] let us first remove it from the overall model used to simulate data in the 400−1000 nm range. The model now just simulates spectral evolution and is similar in spirit to methods used to globally reconstruct time-resolved Stokes shift fluorescence data.[19]

The spectral shift of the *s* band is described by an exponential correlation function

$$\upsilon_s(t) = \upsilon_s(\infty) + (\upsilon_s(0) - \upsilon_s(\infty))e^{-t/\tau_{corr}} \qquad (1)$$

where $\upsilon_s(t)$ represents the frequency of the peak absorption of the electron *s* band as a function of time and τ_{corr} represents the characteristic solvation time.[30] The overall functional form of the solvated electron spectrum employed is due to Jou and Freeman.[53] The low-energy side of the spectrum is represented by a Gaussian function and the high-energy side by a Lorentzian. This analytic form accurately describes the equilibrium solvated electron spectrum over a variety of temperatures.[53] Further, it has been noted that the energy width and overall shape of the

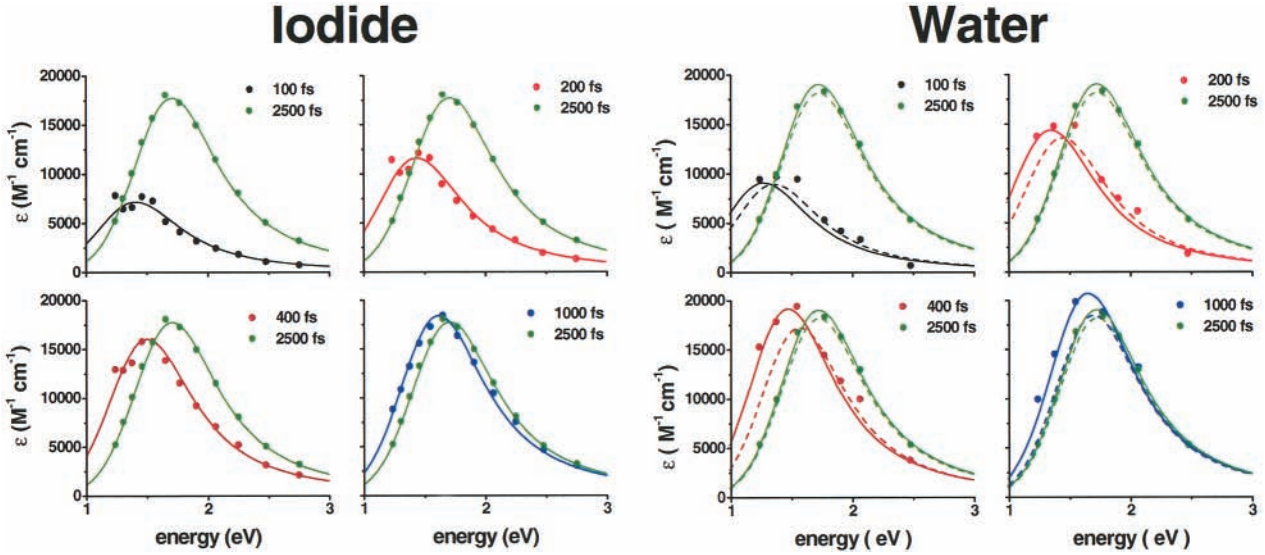

Figure 6. The transient spectra of photoelectrons undergoing relaxation after ejection from I^- (left) and from H_2O (right) in liquid water. Spectra are plotted in energy units. (left) At early times, the experimental data (circles) shows evidence for two peaks, one in the IR which is incompletely resolved in the spectral range studied and a main band that blue shifts with time toward its equilibrated value of 1.73 eV. The global fit (solid) shows a constant width band shifting due to the solvation of the electron. The parameters are $\tau_{corr} = 850$ fs, $\upsilon(0) - \upsilon(\infty) = 0.36$ eV, and $k_p^{-1} = 225$ fs. The additional IR feature is not reproduced by the global fit. (right) The experimental data points show a single band with a larger initial shift. The spectral intensity on the red side of the transient spectrum is not reproduced in the first picosecond by the global fit assuming constant oscillator strength and constant width (dashed line; parameters are $\tau_{corr} = 350$ fs, $\upsilon(0) - \upsilon(\infty) = 0.5$ eV, and $\tau_{rise} = 155$ fs). Including an extra exponential decay component for ϵ_{max}, or equivalently for $\Omega_g(t)$, yields an improved fit (solid line; see text for parameters).

solvated electron spectrum in water is remarkably stable with respect to temperature.[4,55,73] Thus, we follow Jay-Gerin and coworkers and assume that the Gaussian and Lorentzian half-widths W_G and W_L, respectively, and the peak extinction ϵ_{max} are constants over the spectral evolution and use the literature values for equilibrium solvated electrons in H_2O rather than D_2O: $W_G = 0.355$ eV, $W_L = 0.489$ eV, $\upsilon_s(\infty) = 1.725$ eV, and $\epsilon_{max} = 19\,000$ M^{-1} cm^{-1}.[53] The time-dependent spectral function thus consists of a moving, constant shape and constant oscillator strength band with the center frequency $\upsilon_s(t)$:

$$\epsilon(\upsilon,t) = \epsilon_{max}[\exp((-\ln\ 2\ (\upsilon - \upsilon_s(t))^2)/W_G^2] \qquad \text{for } \upsilon \le \upsilon_s(t)$$

$$\epsilon(\upsilon,t) = \epsilon_{max}\left[\frac{1}{\left(\frac{\upsilon - \upsilon_s(t)}{W_L}\right)^2 + 1}\right] \qquad \text{for } \upsilon \ge \upsilon_s(t) \qquad (2)$$

For a global fit, the spectral evolution function must be combined with the population dynamics to reproduce all aspects of the data. This comprises a trapping time, or delayed appearance time, for the ejected electron and a survival probability of the electron population from geminate recombination. Both aspects are appropriate only for a given ejection mechanism and ejection length. Thus, we use the survival probability $\Omega(t)$ function for the overall electron population determined in our earlier paper[6] for these systems at the same pump wavelength. This function for electron-OH recombination is

$$\Omega_g(t) = \mathrm{erfc}\left(\frac{r_{xn}}{\sqrt{4D't_g}}\right) + \frac{r_{xn}\exp[-r_{xn}^2/4D'(t+t_g)]}{\sqrt{\pi D'(t+t_g)}} \times \mathrm{erfc}\left(\sqrt{\frac{r_{xn}^2 t}{4D't_g(t+t_g)}}\right) \qquad (3)$$

where the reaction radius is $r_{xn} = 5.7$ Å,[27] the mutual diffusion coefficient is $D' = 0.0007$ Å^2/fs, and for 9.7 eV excitation the mean ejection radius, $\langle r_0 \rangle = (16D't_g/\pi)^{1/2}$, is 15 Å.[6] These parameters are fixed in our global fitting. In addition, a first order appearance time τ_{appear} for the electron is included as a fitting parameter. Overall, the simulated signal is $S(\upsilon,t) = (1 - \exp(-t/\tau_{appear}))\ \Omega_g(t)\ \epsilon(\upsilon,t)$. For electron−iodine recombination, a competitive kinetics equation describes the total population of solvated electrons within and outside a caged pair:[16]

$$\Omega_{SB}(t) = \frac{k_d}{k_d + k_n} + \frac{k_p}{k_d + k_n - k_p} \times \left[\frac{k_p - k_d}{k_p}e^{-k_p t} - \frac{k_n}{k_n + k_d}e^{-(k_d + k_n)t}\right] \qquad (4)$$

For 255 nm resonant excitation, the inverse rate of diffusive escape ($1/k_d$) and inverse nonadiabatic reverse electron-transfer rate ($1/k_n$) are fixed at 70 and 33 ps, respectively.[6] The rate of electron caged pair appearance k_p is allowed to vary to improve the early time match with the experiment. The simulated signal for iodide at probe frequency υ is just given by $S(\upsilon,t) = \Omega_{SB}(t)\ \epsilon(\upsilon,t)$.

V. Results of Global Fitting

With this simple three-parameter ground-state solvation model, our best fit to the thirteen data sets represented in Figure 3a for iodide detachment and six data sets for water in Figure 3b are given as follows: for I^-, $\upsilon_s(0) - \upsilon_s(\infty) = 0.36$ eV and $\tau_{corr} = 850$ fs, $k_p^{-1} = 210$ fs and for water ionization, $\upsilon_s(0) - \upsilon_s(\infty) = 0.5$ eV and $\tau_{corr} = 350$ fs, $\tau_{appear} = 155$ fs. The fits capture the major part of the spectral evolution; however, some details uncovered in the experiment are absent from the simulations resulting from this simple solvation model. The quality of the fit can be assessed by examining spectral cuts at various delay times (solid lines Figure 6(left)). Notice how the thermalization time for the iodide system is more than twice as long, and there is a smaller shift in the iodide system. The figures illustrate that, in particular, excess intensity is found in the

experimental data for both ejection processes on the red side of the spectrum at delay times up to 1 ps. For iodide (Figure 6 (left)), this difference is manifested as what seems to be an independent contribution at 1000 nm (and presumably beyond) that rises and falls more rapidly than the remainder of the signals on the IR side. We note that this ~20% intensity discrepancy is more striking in the time domain between the simulated and the experimental 1000 nm signal. The fact that a separate band at a longer probe wavelength is hinted at in the pure aqueous solution echoes what is seen more convincingly in the water/glycol data (Figure 3c). For aqueous iodide, leaving aside the discrepancy around 1000 nm, the remainder of the overall spectral evolution of the ground-state electron is well-captured by the ground-state solvation model.

For water, the simulated signals are uniformly underestimating the signal intensity and possibly the bandwidth in the first picosecond at probe wavelengths through 800−1000 nm (dashed lines on Figure 6 (right)). Several modifications to the model were attempted to improve this situation, including relaxing the constraint of shape stability by allowing a time-dependent width function on the Gaussian side. We found that in no case could one improve the fit while maintaining the requirement for fixed integrated band strength.[4] If instead one allows additional oscillator strength for the ground-state band over the first picosecond, the primary effect is to add intensity to the 800−1000 nm region. Including a time varying ϵ_{max} into the model with otherwise constant spectral width substantially improves the agreement with the experiment (solid lines on Figure 6 (right)). The best fit parameters are $\tau_{appear} = 200$ fs, $\tau_{corr} = 500$ fs, and $\Delta E_{solv} = 0.56$ eV with 24% additional ϵ_{max} decaying exponentially with time constant 1.5 ps. Hippler and co-workers have suggested that the earliest part of the population decay has been missed by earlier experiments because of the assumption of the separation of time scales for spectral evolution of the electron and recombination.[4,28] This is consistent with our best fit. Instead of requiring additional oscillator strength for the early time electron spectrum, a better explanation is that there is additional population decay phase that is not currently accounted for in the survival probability function (3). We believe it is entirely reasonable to challenge the early phase of the survival probability function resulting from a diffusion-based recombination model. The earliest recombination events occur between electrons ejected to short range where the effects of structured size solvent shells, rather than a structureless continuum, becomes significant. We return to this point in section VI.

Before settling on this conclusion, it is reasonable to ask whether the missing spectral intensity in the infrared for the relaxation of photoelectrons ejected from water can be accounted for by returning to the full model proposed by Jay-Gerin and co-workers, i.e., by reintroducing the possibility of an excited state (*p*-state) electron in the model (as in Figure 5c). The iodide data indeed implies that a precursor state may be observed, and if a precursor state was involved in both ejection processes, this would account for the very similar trapping times observed in each of our experiments despite the different mechanisms for electron formation. For completeness, we attempted a fit to our water photoionization data employing the full model of Jay-Gerin and co-workers,[30] constraining all parameters for the spectral shape of the *p* band to values determined in that study. We find it impossible to reconcile the parameters from Jay-Gerin and co-workers original study with our data. In particular, if a *p*-state electron is directly formed by the photoionized water molecule, the internal conversion time must be substantially shorter than the 410 fs reported by these authors because we see ≤200 fs signal rises throughout the IR and visible. Even allowing the internal conversion time to be reduced to <120 fs, the *p* state does not fill in any significant amount of the missing intensity in the 800−1000 nm range (see Figure 5c). We find it significant that Jay-Gerin and co-workers were forced to include an extra spectral component around 940 nm with a relatively long lifetime of 2 ps to satisfactorily match the data in the 800−1100 nm region. Only when we include this final ad hoc component to our two-state plus solvation fit, we begin to see reasonable agreement with our experimental data.[75] In our fits, this ad hoc component has a slightly higher ($\epsilon \sim 5000$) and a slightly shorter exponential decay (1.5 ps) compared to values reported in ref 30. We note that this spectral component was unassigned by Jay-Gerin and co-workers and these authors were clearly unhappy in their discussion with its inclusion.[30] Gauduel and co-workers also emphasized the need to include an extra peak in this spectral region; they assigned it to an encounter pair absorption on the basis of comparison to ionization in highly acidic solutions.[76,77] However, their (kinetic) model did not include the continuously blue shifting ground state.[30] We agree with Hippler and co-workers that a much better explanation is now available for this extra IR intensity. The additional intensity in this region is due to a missing population decay phase (also characteristic time 1.5 ps), and that either *p*-state electrons were formed in Jay-Gerin and co-workers' study entirely by absorption of an additional 2 eV pump photon or the $p \rightarrow s$ internal conversion time is much shorter than 400 fs and was obscured by the time resolution available to these workers. If *p*-state electrons, or in fact any precursor state of the electrons,[63] are directly formed in our experiments on the photoionization of water, their lifetime is shorter than 150 fs.[2,44,45,64,78,79] Clearly, any definitive comment on whether a *p*-state electron is directly produced in the two-photon ionization of water cannot be based alone on the recent studies employing a restricted range of probe wavelengths, reported here and elsewhere.[3,4] A very recent study published by Laenen et al. provides evidence for precursors absorbing in the mid-IR after two-photon ionization of both H_2O and D_2O,[63] but these transients do not spectrally coincide with the features previously assigned as an electron *p* state.[30] It would seem that a full analysis of these long probe wavelength studies is mandatory while adequately including the ground-state relaxation. We emphasize that substantial absorption is observed within 200 fs even in the bluest wing of the ground-state spectrum.

VI. Discussion

Our results target the overall thermalization process of hot electrons injected into the aqueous environment from two sources: direct CTTS detachment of iodide and water ionization above the threshold of the conduction band of the liquid. The global-fitting results suggest different relaxation time scales and overall energy dissipation for the two pathways. Moreover, on the addition of 17% mole fraction of ethylene glycol to the water solvent, iodide photodetachment is characterized by a slower solvation time for ground-state electrons but faster rise times at all probe wavelengths and strong evidence for a longer wavelength absorbing precursor. A precursor species is hinted at in iodide photodetachment in pure water but, ironically, is not observed within our spectral window for the two-photon water data where its inclusion in the ionization mechanism has been long-standing.[26,60−62] In this section, we address the differences in ejection mechanisms leading to these observations.

Water Ionization. We initially performed experiments for the water system to provide a benchmark for an ejection process that leads to electrons ejected far from their initial site. The relaxation dynamics are expected to reflect the rearrangement of solvent shells made up entirely of H_2O molecules. However, the ionization of water has itself recently come under increased experimental scrutiny. First, the mechanism for electron ejection may be rather complex and depend significantly on excitation energy.[21,23,80] It is proposed that there is a changeover in mechanism as the total excitation energy is increased up to 12 eV.[3,21,23,31,80,81] The precise mechanisms are still under debate, but it appears that between 9.3 and 10 eV, although there is sufficient energy to reach the conduction band, there is a competition between an ejection pathway that leads to quasifree electrons in the conduction band and an "indirect" ionization mechanism.[3] We have indeed observed that the solvated electron signal increases markedly in our apparatus when the two-photon excitation energy is increased from 9.3 (266 nm) to 9.7 eV (255 nm). In this context, our mapping of the relaxation dynamics with the highest time resolution to date over 500−1000 nm after excitation at 9.7 eV is of some interest in this arena. Second, the involvement of the *p* state, has recently been called into question; on one hand, some argue that no additional transient states are required to explain the relaxation[4] and, on the other, that new precursors rather than the cavity model *p* state are observed in the mid-IR before the appearance of the ground-state electron.[63] Finally, it has recently been reported that the lifetime of the *p*-state electron is considerably shorter (as low as 50 fs) than previously accepted.[2,64]

Pepin et al. were the first to fully characterize the spectral evolution of the electron ejected from water;[30] however, the total energy deposited in the pump step is uncertain. The authors suggest that 5×2 eV are absorbed based on the recombination profile; however, it is possible that electrons trapped after ejection can absorb one or more photons from the long pump pulse and become further excited. This would allow the introduction of *p*-state electrons that are not formed in the ejection process itself. Recent studies have instead employed two-photon UV excitation.[3,4,23,28,31−33,80,82] However, only two complete multiprobe wavelength studies have been reported which consider the relaxation of the ejected electron.[3,4] Both Madsen et al.[3] and Hertwig et al.[4] used 2×4.65 eV to ionize H_2O. The tail end (>1 ps) of the rapid relaxation of the electron is recovered from pump−probe data by Madsen et al.; their experiment is limited by the large GVM (∼0.8 ps) between pump and probe because of the 1.8 mm path length.[3] However, these authors fully recovered and separated the geminate recombination dynamics and spectral evolution by fitting transient spectra at each delay with absolute absorbances. They modeled the observed spectral evolution from 1 ps onward with the literature temperature-dependent spectral form of the thermally equilibrated ground-state electron.[53] They found that the data could be successfully reproduced with a 30 K temperature shift and a 700 fs exponential time constant. In contrast, Hertwig et al. performed an experiment with similar time resolution and probe spectral coverage to ours and captured a much larger spectral evolution, 0.5 eV blue shifting and an approximate 300 fs time constant.[4] Our experimental results are in good agreement despite the slightly higher excitation energy used in our experiments (9.7 vs 9.3 eV). The relaxation observed in the data reported here and in the results of Hertwig et al. corresponds to an additional 170 K cooling taking place before 1 ps that was not resolved in the experiment of Madsen et al.

As discussed in section V, we are also in agreement with the main conclusions of Hertwig et al. First, to best fit the observed transient spectra, an additional population decay phase is necessary. This population decay is assigned to an early geminate recombination phase that has been ignored by other workers who typically start fitting the population decay phase after 1 ps[23,31,32] and can be attributed to deficiencies in the recombination model at the earliest times.[6] An additional 25% of electron population is implicated over and above that accounted for with the diffusion-limited geminate recombination model (eq 3). We have reported a fraction escaping diffusive recombination as ∼60%, in close agreement with others.[23,80] Thus, adding the amplitude of the new recombination phase occurring in parallel with electron solvation (0.25/1.25) to the recombination fraction (0.4/1.25) fit by the diffusive recombination model,[6] we arrive at a revised total recombination fraction of 52%, with only 48% of electrons escaping.

It is reasonable to question whether such a fast recombination phase is possible, particularly in light of the finding that electrons in contact with a halogen atom undergo rather slow recombination,[6] in agreement with simulations.[13,16] It is usually assumed in the photoionization of liquid water that photoelectrons are ejected into a distribution of radii from the parent; therefore, a fraction of the electrons is ejected to short range. The diffusive reactive pair model treats any electrons ejected within the reaction radius as immediately recombining.[6] The survival probability is renormalized to unity to ignore this fraction. In reality, electrons ejected within this radius (i.e., trapped in the first or second solvent shell surrounding the ionized parent molecule) will recombine with OH or H_3O^+ in a finite time determined by the nonadiabatic transition probability. Recent electron quenching experiments in our laboratory show that at high concentrations of added H_3O^+ ions (∼5 M), where every solvated electron is likely in close proximity to a quencher, the solvated electron population decays exponentially with a time constant of only a few picoseconds.[83] This nondiffusive (or "static") quenching result suggests that the nonadiabatic electron-transfer rate for a H_3O^+:e^- contact pair is indeed very fast. The H_3O^+ reaction is actually not considered diffusion-limited, whereas the reaction with OH radical is.[32] We therefore believe the fast geminate recombination phase recovered in our analysis is reasonable because both OH and H_3O^+ species are potentially available to the short-range ejected electron.

Second, Hertwig et al. also argue that no additional signals due to an excited electron state are observed at early times and speculate that *p*-state formation is not taking place in the ionization step.[4] Within the time and spectral window where our experiments recover signals, we also find no need to include a *p* state (or any precursor state) to model our data for water ionization. Our global analysis of all data sets indicates a hot electron is formed in the ground state in ∼200 fs and undergoes ∼ 0.5−0.6 eV blue shifting with a characteristic time ∼500 fs. Either a *p* state is not an intermediate in the electronic relaxation of the ejected electron or, if it is formed, it must have a much shorter lifetime to internal conversion than previously assumed.[30] However, of the experiments at around 9.5 eV excitation (including this one), only the recent report from Laenen et al. has employed probes further red than 1050 nm.[63] This recent experiment observes rapidly decaying (<200 fs) transients at 1600 and 2900 nm, but instead of attributing these to a cavity *p* state, based on their spectral shifts in D_2O, the authors assign them as different short-lived precursors.[63]

The solvation time for the ground-state electron that we have derived is in good agreement with the slow (diffusive) solvation time for the response of liquid water to a photoexcited dye probe.[18,20] The latter may be associated with the Debye

relaxation time in a dielectric model of water relaxation.[84] We feel it is now well-established that diffusive solvent relaxation around the ground-state electron is the predominant relaxation process observed from 200 to 4000 fs after photoejection. It is interesting to compare this result to the ground-state solvation time extracted from pump−probe experiments on equilibrated electrons.[45,46] Although the experiments starting with equilibrated electrons can be performed at higher time resolution given both the experimental wavelengths and minimal GVM between pump and probe pulses, their interpretation is complicated by the requirement of unraveling overlapping ground-state bleach, excited-state absorption, and stimulated emission signals. The most recent report by Barbara and co-workers observes spectral evolution on 50 fs, ~300 fs, and 1 ps time scales.[1] These authors give arguments based on the expected pump saturation behavior and experimental results where two pump photons are absorbed, along with comparisons to nonadiabatic molecular dynamics simulations,[78,79] to justify a preference for assigning the short time scale dynamics to solvent motions around the photoexcited *p* state with the $p \rightarrow s$ transition assigned as one of the slower recovered components.[1] Nonadiabatic molecular dynamics simulations predict a 350 fs nonadiabatic relaxation time scale for an equilibrated *p* state once the effect of decoherence is taken into account in the simulation.[79,85] Recent conclusions from Wiersma's group based on 5 fs pump−probe experiments[2,64] disagree and argue strongly for assigning the relaxation of the photoexcited *p* state in three phases as follows: (a) a 55 fs depopulation of the excited *p* state to form a hot ground state, (b) a phase between 100 and 300 fs where some energy relaxation takes place (as water librational modes transfer energy to collective translational modes), and (c) pure translational relaxation with a characteristic 1.2 ps time scale.[64] A total of ~0.5 eV is released in the two ground-state relaxation phases, although the 1.2 ps phase is dominant.[64] It is certainly reasonable that if the *p* state is eventually implicated in the relaxation of photoejected electrons the $p \rightarrow s$ internal conversion rate may vary between an electron undergoing nonadiabatic transition in a preestablished solvent cavity, which is probed in the equilibrated electron pump−probe experiments, and a freshly ejected electron rapidly establishing a new cavity in the solvent.[78]

Iodide Detachment. We now turn our attention to the comparison of the relaxation of the photoelectron resulting from detachment of iodide with that after water ionization. Our results for I^- are suggestive of a differing excess energy dissipated by the solvent and a differing environment for the relaxation dynamics. The global fits for I^- detachment in pure water yield 0.36 eV as the extent of the blue shift of the transition energy with a solvation time of 850 fs. Except for evidence of an additional absorption at the longest probe wavelengths, the complete 13-probe data set may be fit with a constant width and constant oscillator strength ground-state spectrum undergoing continuous blue shifting. The spectral evolution describes the response of the electron's environment to accommodating the new separated charge. Our analysis of the geminate recombination kinetics after CTTS detachment indicates that the electron is ejected to very short range and may form a caged pair with the nascent iodine radical with a lifetime of ~20 ps.[6] The occurrence of caged pairs for electrons produced by low-energy photodetachment is supported by evidence from theoretical simulations[13,16] and similar modeling of experimental data on Na^-.[41,42] Therefore, the observed difference in relaxation time scales for the ejected electron is consistent with a rather different environment surrounding the ejected electron, e.g., with the presence of an iodine atom in the first solvent shell. We note that no changes to the geminate recombination model[6] are required with the more comprehensive global fit, which unlike the H_2O ionization case appears to show no "immediate" recombination phase.

However, in analyzing our data we have assumed the electron detached from iodide at 10 ps has an absorption spectrum identical to a fully equilibrated solvated electron in water.[53] Indeed, if this assumption is in error, the overall form of the intensity distribution in the contour plots will change markedly. For water ionization, the assumption seems clearly justified based on the length scale of the electron ejection and previous reports.[3] However, if the parent iodine atom is at close range to the ejected electron within this time frame, it is reasonable to question whether there is an interaction that is sufficient to substantially perturb the absorption spectrum of the solvated electron. We justify our assumption that this perturbation is minimal by statements by both groups performing quantum molecular dynamics simulations on the photodetachment process and observing caged halogen−electron pairs.[13,16] Further, from our experiments, we do not observe any spectral evolution from 10 ps out to 400 ps by which time all electrons should have escape the influence of the iodine atom.

The data for iodide detachment in the glycol/water environment provides additional information. Clearly, the most interesting result in the mixed solvent data is the additional evidence for a second transient absorption band at long wavelengths that now comes squarely into our spectral window. Thus, whereas in aqueous iodide detachment we saw only a suggestion of a separate absorption band for the early-time detached electron, significantly more intensity is now observed at 1000 nm.[86] In addition, continuous spectral evolution of the ground-state band is once again observed. To extract the latter, we explicitly modeled the early-time absorption by inclusion of a separate precursor electronic state and fit the mixed solvent data (Figure 3c) using a two-state model with ground-state solvation (as in Figure 5c). We find a reasonable fit with the precursor lifetime of 220 fs and a ground-state solvation time and shift of 1.5 ps and 0.25 eV, respectively. Therefore, the solvation response is slowed by almost a factor of 2 with the addition of ethylene glycol molecules to the solvent environment. In pursuing this two-state fit, the precursor state was modeled as a *p* electron with all parameters taken from ref 30 except the position of *p*-band center, which after application of the same solvent blue shift[68] for 17% mole fraction glycol as for equilibrated ground-state band was placed at 1100 nm. The use of the *p*-state parameters is arbitrary and is based on a lack of additional information about this early time spectral component; we emphasize that no assignment of the early spectral component to an absorption of a *p*-state electron can be inferred from our experiment.

Given the smaller excess energy for the ejected photoelectron (Figure 1) after one-photon detachment, it perhaps is not surprising that the extent of ground-state cooling is smaller than observed after two-photon solvent ionization. It is however surprising, given the small energy gap between the prepared CTTS state and a relaxed solvated electron, that a separate absorption band, suggesting a precursor state for the detached electron, be observed. This is particularly puzzling given the prediction from quantum/classical simulations of an adiabatic evolution from the lowest CTTS state to the ground state of the separated electron.[13,16,87] For example, Sheu and Rossky considered the possibility of conversion from the lowest CTTS state for aqueous iodide into a *p*-state electron and concluded that it was prohibited because of energetic considerations: the

calculation indicated a ~2 eV uphill energy gap for this conversion.[11] However, experimental evidence has recently been presented for a precursor absorption in the photodetachment of aqueous $[Fe(CN)_6]^{4-}$,[88] a system whose initial state has been assigned as CTTS and whose energy gap with respect to the equilibrated solvated electron is similar.[39] Cognizant of the checkered history of assigning additional states as early time precursors in the ionization of water, we believe that the assignment of this additional absorption near 1000 nm is perilous and we leave this issue open pending additional experiments. Instead, let us restate the key observations relating to this feature for iodide detachment: At 1000 nm, substantial additional absorbance is observed at very early times in the mixed solvent that is not accounted for by a continuous spectral shifting of the ground-state spectrum. A smaller additional absorbance at the same wavelength is observed for the detached electron in purely aqueous iodide solutions. The extra absorption component in the mixed solvent decays very rapidly (~200 fs). Characterization of the magnitude, but not the decay of this component, is dependent on our assumption of matching the 15 ps spectrum to the literature equilibrated electron spectrum.[53,68] The observed strengthening of intensity of this spectral component for the glycol/water mixture is consistent with the blue shift observed for both the iodide ground → CTTS state transition and the ground-state solvated electron band.[47,89] However, to complicate the picture, in addition to this spectral component which might be identified with a precursor electron state, our experiments also observe a fast decaying transient (≤50 fs) around time zero (Figure 4).

Figure 4 shows the spectrum of the zero-delay transient; this may be the *excited-state spectrum* of the iodide ion, although the extremely short lifetime of the experimental transient makes us cautious in our assignment as such. It is worth noting that Figure 4 shows some similarity to a comparable graph in the paper by Long et al.,[71] assigned by those authors as an absorption by the lowest CTTS state formed after internal conversion from the higher-lying prepared iodide state. One-photon allowed transitions from the lowest CTTS state should correspond to an $s \rightarrow p$ promotion of the CTTS electron or transitions to the continuum. Let us consider prior assignments relevant to higher excited states of I^-(aq). Additional CTTS states for aqueous iodide were observed in the ground-state absorption spectrum by Fox and Hayon.[90] However, selection rules dictate that these transitions involve further *s* and *d* symmetry excited states, and thus transitions from the first exited CTTS state to these levels are symmetry forbidden. The onset of the continuum for aqueous iodide is estimated at 7.0 eV above the ground state,[72] and thus transitions to the continuum in the excited-state spectrum would be possible from 550 nm toward the blue. Sheu and Rossky simulated the transient spectrum of the lowest CTTS state that indicated an $s \rightarrow p$ CTTS band at similar transition energy to the band predicted for the separated electron product at longer times.[11] This may account for the transient intensity at 750 nm. However, in simulations of Cl^- detachment, the pair of states involved in this $s \rightarrow p$ transition adiabatically evolve into the *s* and *p* states of the separated electron and the simulations show this band should undergo continuous blue shifting on evolution from CTTS state to separated electron.[16] In other words, the separation is continuous with the relaxation dynamics of the solvent shell surrounding the chlorine/electron pair and thus the pump−probe spectrum is simulated to evolve continuously.[16] The main difference between the simulations for iodide and chloride detachment is the intermingling of *d*-symmetry one-electron states within the lowest CTTS manifold, which are actively involved in the detachment mechanism.[13] Therefore, it is reasonable that for iodide detachment, within the crucial period 100−500 fs indicated in the simulations where the electronic wave function is strongly mixed, the $s \rightarrow p$ band temporarily disappears to reappear later once the electron is separated and the final orbital symmetry is established.[13] Given the change in the symmetry of the occupied one-electron state during this period, it is certain that the available oscillator strength for absorption transitions changes. We suggest this proposal may account for the zero-delay feature assignment of the CTTS excited state absorption as being distinct from complete spectral evolution of the electron spectrum. It is worth noting that some of the widths of the features indicated in Figure 4 seem unreasonably narrow for the proposed transitions; however, the error bar on each absorbance data point is rather large given the sensitivity to correctly fitting the shape of the time-zero transient.

It is clear that some rather interesting detachment dynamics are going on in the first 200 fs after excitation, in particular on the infrared side of the spectrum. Not only does confirmation of the precursor state at 1000 nm need to be tested by experiments further into the IR but an explanation for the spectrally distinct transient absorption around time zero is required. Current experiments in our lab using thinner water jets will allow us to make full use of our <50 fs resolution to resolve some of these outstanding questions. New simulations exploring the earliest phase of the detachment process would be extremely valuable in this regard. Time-resolved fluorescence experiments have been suggested as a means to unambiguously assign the various transient electronic species suggested at early times, whose signatures in transient absorption spectrally overlap.[10,11] We plan to try such experiments, exploiting the <100 fs resolution of the fluorescence upconversion technique.[18]

We bring the discussion for iodide detachment to a close by making direct comparisons to the situation recently explored experimentally and theoretically in gas-phase clusters. Johnson and co-workers have shown that small water clusters binding an iodide ion exhibit bound states in their absorption spectra that lie within the detachment continuum.[8] As the number of water molecules in the cluster increases, the bound states become increasingly stabilized with respect to the detachment threshold. Johnson and co-workers suggest these excited dipole-bound states are precursors to the bulk CTTS state. Ab initio calculations have shown, however, that the lowest energy configuration for $I^-(H_2O)_n$ clusters is for the iodide to sit on the surface rather than break up the hydrogen bonding network.[56,91] Very recently, three groups have computed the cluster CTTS-analogue excited state via ab initio methods.[17,56,57] The dipole-bound state has a considerably extended electronic wave function, which is highly asymmetric about the iodine.[17,57] In comparison, the bulk CTTS state of halides are believed to have a spherically symmetrical wave function centered on the iodine which is trapped by the preexisting polarization of the surrounding water network,[13,47] and that network cannot have a large fixed net dipole. It is interesting that Chen and Sheu find a bound excited state for an *interior* iodide cluster, where the water cluster (in the absence of the iodide) has only a small permanent dipole.[17]

Despite these differences in the particular character of the iodide excited state, it is valuable to compare our dynamical results in the bulk phase with recent time-resolved photoelectron spectroscopy of hydrated iodide clusters from Neumark and co-workers.[9] In these experiments, clusters are excited with a pump pulse into the dipole-bound state and a probe pulse monitors the photoelectron spectrum of the excited cluster at various

subsequent delay times. The time-resolved photoelectron spectroscopy experiment determines the appearance of a state in the cluster within 200 fs in $I^-(D_2O)_{4-6}$ and ~100 fs for $I^-(H_2O)_{4-6}$. This is followed, for clusters with five or more waters, by a change in the photoelectron spectrum over ~500 fs that is assigned to relaxation of the water network around a separated electron. The energy shift in the photoelectron spectrum as the solvated electron cluster rearranges is 0.3 eV.[9] The time scale for the waters to rearrange their positions and orientations and the magnitude of the nuclear relaxation are very comparable to the numbers we report. This agreement is intriguing, but several questions remain: Is the initially observed state in the cluster experiment the charge-separated state or the dipole-bound state itself? Does the first 200 fs induction time correspond to the destruction of the CTTS-like state and the formation of the separated pair followed by nuclear rearrangement in the cluster (or isomerization)? An alternative assignment is made in the work of Neumark and co-workers: the CTTS state is the carrier of the initial transient photoelectron signal, and the isomerization is continuous from the separation of the charge through to the relaxation of the trapped electron. Neumark and co-workers assignment implies that a quasistable electron−iodine contact pair is formed in the cluster, as we have suggested for detachment in the bulk.[6] However, in the cluster, the iodine atom is on the outside of the cluster, and so there is well-defined direction for the electron to separate.

VII. Conclusion

We have presented spectral maps of the relaxation dynamics of ejected electrons based on 50 fs pump−probe experiments in three different systems. It is clear from the results and global fitting that the photoelectrons ejected via multiphoton ionization and below threshold photodetachment lead to different characteristic relaxation. The relaxation is primarily identified as ground-state solvation by diffusive rearrangement of the solvent surrounding the nascent electron. The time scale is slower, and the extent of ground-state solvation is smaller for iodide detachment. This suggests differences in local environment for the electron undergoing relaxation and differing amounts of available energy to the ground-state electron formed. Comparisons with quantum classical molecular dynamics simulations are encouraging for the appearance time of the ground-state electron, but the detailed spectral evolution is rather more complex at early times in the experimental data. It is interesting that, despite the energetics suggesting a variety of precursor states of the ejected electron, including the cavity model *p* state, being accessible only to the two-photon ionization pathway, modeling of our results for the ionization of water does not require additional states, but a precursor state is suggested by the results for the iodide system. This suggests a different pathway for electrons to reach their electronic ground state in the two-ejection mechanisms. By extending the probe spectral window, we are currently performing experiments to fully address this issue.

Acknowledgment. We thank Maxim Pshenichnikov for bringing our attention to ref 64 and 67 and Ben Schwartz and Paul Barbara for useful conversations. This research is supported by grants from the National Science Foundation (CHE-9817835) and by the donors of the Petroleum Research Fund administered by the American Chemical Society. S.E.B. is a recipient of the Camille and Henry Dreyfus Foundation New Faculty Award, a Cottrell Scholar of Research Corporation, and a David and Lucile Packard Foundation Fellow in Science and Engineering.

References and Notes

(1) Yokoyama, K.; Silva, C.; Son, D. H.; Walhout, P. K.; Barbara, P. F. *J. Phys. Chem. A* **1998**, *102*, 6957.
(2) Baltuska, A.; Emde, M. F.; Pshenichnikov, M. S.; Wiersma, D. A. *J. Phys. Chem. A* **1999**, *103*, 10065.
(3) Madsen, D.; Thomsen, C. L.; Thogersen, J.; Keiding, S. *J. Chem. Phys.* **2000**, *113*, 1126.
(4) Hertwig, A.; Hippler, H.; Unterreiner, A. N. *Phys. Chem. Chem. Phys.* **1999**, *1*, 5633.
(5) Assel, M.; Laenen, R.; Laubereau, A. *J. Chem. Phys.* **1999**, *111*, 6869.
(6) Kloepfer, J. A.; Vilchiz, V. H.; Lenchenkov, V. A.; Germaine, A. C.; Bradforth, S. E. *J. Chem. Phys* **2000**, *113*, 6288.
(7) Ayotte, P.; Johnson, M. A. *J. Chem. Phys.* **1997**, *106*, 811.
(8) Serxner, D.; Dessent, C. E. H.; Johnson, M. A. *J. Chem. Phys.* **1996**, *105*, 7231.
(9) Lehr, L.; Zanni, M. T.; Frischkorn, C.; Weinkauf, R.; Neumark, D. M. *Science* **1999**, *284*, 635.
(10) Sheu, W.-S.; Rossky, P. J. *Chem. Phys. Lett.* **1993**, *213*, 233.
(11) Sheu, W.-S.; Rossky, P. J. *Chem. Phys. Lett.* **1993**, *202*, 186.
(12) Sheu, W.-S.; Rossky, P. J. *J. Am. Chem. Soc.* **1993**, *115*, 7729.
(13) Sheu, W.-S.; Rossky, P. J. *J. Phys. Chem.* **1996**, *100*, 1295.
(14) Borgis, D.; Staib, A. *Chem. Phys. Lett.* **1994**, *230*, 405.
(15) Borgis, D.; Staib, A. *J. Chem. Phys.* **1996**, *104*, 4776.
(16) Staib, A.; Borgis, D. *J. Chem. Phys.* **1996**, *104*, 9027.
(17) Chen, H.-Y.; Sheu, W.-S. *J. Am. Chem. Soc.* **2000**, *122*, 7534.
(18) Jimenez, R.; Fleming, G. R.; Kumar, P. V.; Maroncelli, M. *Nature* **1994**, *369*, 471.
(19) Horng, M. L.; Gardecki, J. A.; Papazyan, A.; Maroncelli, M. *J. Phys. Chem.* **1995**, *99*, 17311.
(20) Lang, M. J.; Jordanides, X. J.; Song, X.; Fleming, G. R. *J. Chem. Phys.* **1999**, *110*, 5884.
(21) Bartels, D. M.; Crowell, R. A. *J. Phys. Chem. A* **2000**, *104*, 3349.
(22) Chen, R. H.; Avotinsh, Y.; Freeman, G. R. *Can. J. Chem* **1994**, *72*, 1083.
(23) Crowell, R. A.; Bartels, D. M. *J. Phys. Chem.* **1996**, *100*, 17940.
(24) Gauduel, Y.; Pommeret, S.; Antonetti, A. *J. Phys.: Condens. Matter* **1990**, *2*, SA171.
(25) Gauduel, Y.; Pommeret, S.; Migus, A.; Antonetti, A. *Chem. Phys.* **1990**, *149*, 1.
(26) Gauduel, Y.; Pommeret, S.; Migus, A.; Antonetti, A. *J. Phys. Chem.* **1989**, *93*, 3880.
(27) Goulet, T.; Jay-Gerin, J.-P. *J. Chem. Phys.* **1992**, *97*, 5076.
(28) Hertwig, A.; Hippler, H.; Unterreiner, A. N.; Vohringer, P. *Ber. Bunsen-Ges. Phys. Chem.* **1998**, *102*, 805.
(29) Lu, H.; Long, F. H.; Eisenthal, K. B. *J. Opt. Soc. Am. B* **1990**, *7*, 1511.
(30) Pepin, E.; Goulet, T.; Houde, D.; Jay-Gerin, J.-P. *J. Phys. Chem. A* **1997**, *101*, 4351.
(31) Sander, M. U.; Luther, K.; Troe, J. *Ber. Bunsen-Ges. Phys. Chem.* **1993**, *97*, 953.
(32) Thomsen, C. L.; Madesen, D.; Keiding, S. R.; Thogersen, J.; Christiansen, O. *J. Chem. Phys.* **1999**, *110*, 3453.
(33) Peon, J.; Hess, G. C.; Pecourt, J.-M. L.; Yuzawa, T.; Kohler, B. *J. Phys. Chem. A* **1999**, *103*, 2460.
(34) Kloepfer, J. A.; Vilchiz, V. H.; Lenchenkov, V. A.; Bradforth, S. E. *Chem. Phys. Lett.* **1998**, *298*, 120.
(35) Long, F. H.; Shi, X.; Lu, H.; Eisenthal, K. B. *J. Phys. Chem.* **1994**, *98*, 7252.
(36) Lu, H.; Long, F. H.; Bowman, R. M.; Eisenthal, K. B. *J. Phys. Chem.* **1989**, *93*, 27.
(37) Gauduel, Y.; Gelabert, H.; Ashokkumar, M. *Chem. Phys.* **1995**, *197*, 167.
(38) Assel, M.; Laenen, R.; Laubereau, A. *Chem. Phys. Lett.* **1998**, *289*, 267.
(39) Lenchenkov, V. A.; Vilchiz, V. H.; Kloepfer, J. A.; Bradforth, S. E. *Chem. Phys. Lett.* **2001** submitted for publication.
(40) Pommeret, S.; Naskrecki, R.; Meulen, P. v. d.; Menard, M.; Vigneron, G.; Gustavsson, T. *Chem. Phys. Lett.* **1998**, *288*, 883.
(41) Martini, I.; Barthel, E.; Schwartz, B. J. *J. Chem. Phys.* **2000**, *113*, 11245.
(42) Barthel, E. R.; Martini, I.; Schwartz, B. J. *J. Chem. Phys.* **2000**, *112*, 9433.
(43) Wang, Z.; Shoshana, O.; Ruhman, S. In *Ultrafast Phenomena XII*; Elsaesser, T., Mukamel, S., Murnane, M. M., Scherer, N. F., Eds.; Springer-Verlag: Berlin, Germany, 2001.
(44) Alfano, J. C.; Walhout, P. K.; Kimura, Y.; Barbara, P. F. *J. Chem. Phys.* **1993**, *98*, 5996.
(45) Silva, C.; Walhout, P. K.; Yokoyama, K.; Barbara, P. F. *Phys. Rev. Lett.* **1998**, *80*, 1086.
(46) Kummrow, A.; Emde, M. F.; Baltuska, A.; Pshenichnikov, M. S.; Wiersma, D. A. *J. Phys. Chem. A* **1998**, *102*, 4172.

(47) Blandamer, M.; Fox, M. *Chem. Rev.* **1970**, *70*, 59.
(48) Jortner, J.; Levine, R.; Ottolenghi, M.; Stein, G. *J. Phys. Chem.* **1961**, *65*, 1232.
(49) Jortner, J.; Ottolenghi, M.; Stein, G. *J. Phys. Chem.* **1963**, *67*, 1271.
(50) Tran, V.; Schwartz, B. *J. Phys. Chem. B* **1999**, *103*, 5570.
(51) Okazaki, K.; Idriss-Ali, K. M.; Freeman, G. R. *Can. J. Chem.* **1984**, *62*, 2223.
(52) Chandrasekhar, N.; Krebs, P. *J. Chem. Phys.* **2000**, *112*, 5910.
(53) Jou, F.-Y.; Freeman, G. R. *J. Phys. Chem.* **1979**, *83*, 2383.
(54) Jou, F.-Y.; Freeman, G. R. *Can. J. Chem.* **1979**, *57*, 591.
(55) Tuttle, T. R.; Golden, S. *J. Phys. Chem.* **1991**, *95*, 5725.
(56) Majumdar, D.; Kim, J.; Kim, K. S. *J. Chem. Phys.* **2000**, *112*, 101.
(57) Vila, F. D.; Jordan, K. D. *Abstr. Pap. Am. Chem. Soc. Part II* **2000**, *220*, PHYS 375.
(58) Coe, J. V.; Earhart, A. D.; Cohen, M. H.; Hoffman, G. J.; Sarkas, H. W.; Bowen, K. H. *J. Chem. Phys.* **1997**, *107*, 6023.
(59) Han, P.; Bartels, D. *J. Phys. Chem.* **1990**, *94*, 5824.
(60) Migus, A.; Gauduel, Y.; Martin, J. L.; Antonetti, A. *Phys. Rev. Lett.* **1987**, *58*, 1559.
(61) Long, F. H.; Lu, H.; Eisenthal, K. B. *Phys. Rev. Lett.* **1990**, *64*, 1469.
(62) Webster, F. J.; Schnitker, J.; Friedrichs, M. S.; Friesner, R. A.; Rossky, P. J. *Phys. Rev. Lett.* **1991**, *66*, 3172.
(63) Laenen, R.; Roth, T.; Laubereau, A. *Phys. Rev. Lett.* **2000**, *85*, 50.
(64) Baltuska, A. Hydrated Electron Dynamics Explored with 5-fs Optical Pulses, Ph.D. Thesis, University of Groningen, The Netherlands, 2000.
(65) Rips, I.; Silbey, R. J. *J. Chem. Phys.* **1991**, *94*, 4495.
(66) Siddick, E.; Dienes, A.; Knoesen, A. *J. Opt. Soc. Am. B* **1995**, *12*, 1704.
(67) IAPWS "Release on the Refractive Index of Ordinary Water Substance as a Function of Wavelength, Temperature and Pressure"; The International Association for the Properties of Water and Steam, 1997.
(68) Idriss-Ali, K. M.; Freeman, G. R. *Can. J. Chem.* **1984**, *62*, 2217.
(69) Reuther, A.; Laubereau, A.; Nikogosyan, D. N. *Opt. Commun.* **1997**, *141*, 180.
(70) Ekvall, K.; Meulen, P. v. d.; Dhollande, C.; Berg, L.-E.; Pommeret, S.; Naskrecki, R.; Mialocq, J.-C. *J. Appl. Phys.* **2000**, *87*, 2340.
(71) Long, F. H.; Lu, H.; Shi, X.; Eisenthal, K. B. *Chem. Phys. Lett.* **1990**, *169*, 165.
(72) Takahashi, N.; Sakai, K.; Tanida, H.; Watanabe, I. *Chem. Phys. Lett.* **1995**, *246*, 183.
(73) Marbach, W.; Asaad, A. N.; Krebs, P. *J. Phys. Chem. A* **1999**, *103*, 28.
(74) Rossky, P. J.; Schnitker, J. *J. Phys. Chem.* **1988**, *92*, 4277.
(75) We note that the 1-state additional oscillator strength/additional recombination phase fit remains our best fit.
(76) Gauduel, Y.; Pommeret, S.; Migus, A.; Yamada, N.; Antonetti, A. *J. Am. Chem. Soc.* **1990**, *112*, 2925.
(77) Pommeret, S.; Antonetti, A.; Gauduel, Y. *J. Am. Chem. Soc.* **1991**, *113*, 9105.
(78) Schwartz, B. J.; Rossky, P. J. *J. Chem. Phys.* **1994**, *101*, 6902.
(79) Schwartz, B. J.; Rossky, P. J. *J. Chem. Phys.* **1996**, *105*, 6997.
(80) Sander, M. U.; Gudiksen, M. S.; Luther, K.; Troe, J. *Chem. Phys.* **2000**, *258*, 257.
(81) Bernas, A.; Grand, D. *J. Phys. Chem.* **1994**, *98*, 3440.
(82) Reuther, A.; Laubereau, A.; Nikogosyan, D. N. *J. Phys. Chem.* **1996**, *100*, 16794.
(83) Kloepfer, J. A.; Chen, X.; Bradforth, S. E. *J. Chem. Phys.* **2001** manuscript in preparation.
(84) Ronne, C.; Thrane, L.; Astrand, P. O.; Wallqvist, A.; Mikkelsen, K. V.; Keiding, S. *J. Chem. Phys.* **1997**, *107*, 5319.
(85) Schwartz, B. J.; Bittner, E. R.; Prezhdo, O. V.; Rossky, P. J. *J. Chem. Phys.* **1996**, *104*, 5942.
(86) Because only probe wavelengths every 100 nm were recorded for this system, only the 1000 nm data is useful for assessing this band; further data from either side of this wavelength is clearly called for.
(87) Rossky, P. J. Private communication.
(88) Hang, K.; Anderson, N. A.; Asbury, J. B.; Lian, T. In *The Twelfth International Conference on Ultrafast Phenomena XII Technical Digest*; Elsaesser, T., Mukamel, S., Murnane, M. M., Scherer, N. F., Eds.; Springer-Verlag: Berlin, Germany, 2001.
(89) Fox, M. F.; Hayon, E. *Chem. Phys. Lett.* **1974**, *25*, 511.
(90) Fox, M. F.; Hayon, E. *J. Chem. Soc., Faraday Trans. 1* **1977**, *73*, 1003.
(91) Combrazia, J. E.; Kestner, N. R.; Jortner, J. *J. Chem. Phys.* **1994**, *100*, 2851.